

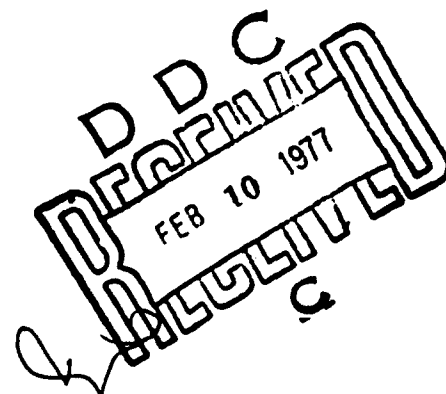
A035462

12

TWO-DIMENSIONAL NUMERICAL MODEL
OF THE NEAR-FIELD FLOW FOR AN
OCEAN THERMAL POWER PLANT.

PART II. SIMULATION OF THE
LOCKHEED BASELINE DESIGN.

SAI-76-625-WA



DISTRIBUTION STATEMENT A

Approved for public release;
Distribution Unlimited



ATLANTA • ANN ARBOR • BOSTON • CHICAGO • CLEVELAND • DENVER • HUNTSVILLE • LA JOLLA
LITTLE ROCK • LOS ANGELES • SAN FRANCISCO • SANTA BARBARA • TUCSON • WASHINGTON

TWO-DIMENSIONAL NUMERICAL MODEL
OF THE NEAR-FIELD FLOW FOR AN OCEAN THERMAL POWER PLANT.
PART II. SIMULATION OF THE LOCKHEED BASELINE DESIGN.

Glyn O. Roberts

Fluid Mechanics Division,
Science Applications, Inc.

and

Steve A. Piacsek* and Juri Toomre**

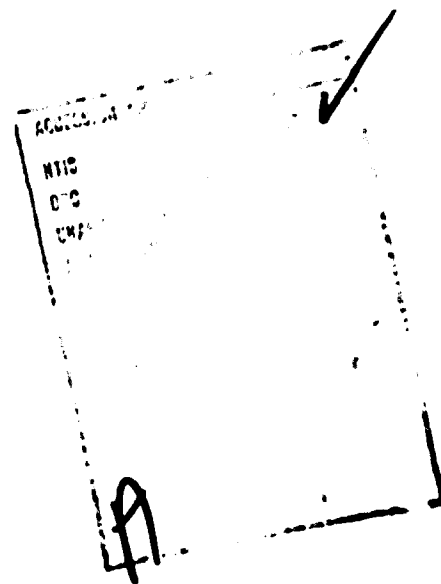
Geophysical Simulation Section, Code 7750
Naval Research Laboratory

SAI-76-625-WA

*Now at Naval Ocean Research and Development Activity

**Department of Astrogeophysics, University of Colorado

Supported by the Ocean Thermal Energy Conversion Program,
Division of Solar Energy, Energy Research and Development
Administration, under ERDA contract E (49-26) 1005.



19 REPORT DOCUMENTATION PAGE		READ INSTRUCTIONS BEFORE COMPLETING FORM	
1. REPORT NUMBER	2. GOVT ACCESSION NO.	3. RECIPIENT'S CATALOG NUMBER	
NRL GFD/OTEC-6-76			
4. TITLE (and Subtitle)		5. TYPE OF REPORT & PERIOD COVERED	
TWO-DIMENSIONAL NUMERICAL MODEL OF THE NEAR-FIELD FLOW FOR AN OCEAN THERMAL POWER PLANT, PART II. SIMULATION OF THE LOCKHEED BASELINE DESIGN.		FINAL, APRIL - NOVEMBER, 1976	
6. AUTHOR(s)		7. PERFORMING ORG. REPORT NUMBER	
GLYN C. ROBERTS, STEVE A. PIACSEK		SAI-76-625-WA	
JURI/TOOMRE OF NRL		8. CONTRACT OR GRANT NUMBER(s)	
		N00014-76-C-0610	
		PRIME CONTRACT	
		E (49-26) 1005	
9. PERFORMING ORGANIZATION NAME AND ADDRESS		10. PROGRAM ELEMENT, PROJECT, TASK AREA & WORK UNIT NUMBERS	
SCIENCE APPLICATIONS, INC. 8400 Westpark Drive McLean, Virginia 22101		NONE	
11. CONTROLLING OFFICE NAME AND ADDRESS		12. REPORT DATE	
NAVAL RESEARCH LAB, CODE 7700A Washington, D.C. 20375		Dec 1976	
14. MONITORING AGENCY NAME & ADDRESS (if different from Controlling Office)		13. NUMBER OF PAGES	
SOLAR ENERGY DIVISION USERDA Washington, D.C. 20545		50	
16. DISTRIBUTION STATEMENT (of this Report)		15. SECURITY CLASS. (of this report)	
UNLIMITED		NONE	
17. DISTRIBUTION STATEMENT (of the abstract entered in Block 20, if different from Report)		15a. DECLASSIFICATION/DOWNGRADING SCHEDULE	
UNLIMITED		N/A	
18. SUPPLEMENTARY NOTES			
NONE			
19. KEY WORDS (Continue on reverse side if necessary and identify by block number)			
OCEAN THERMAL POWER PLANTS THERMAL PLUMES TURBULENCE MODELING STRATIFIED TURBULENCE MODELING			
20. ABSTRACT (Continue on reverse side if necessary and identify by block number)			
<p>This report describes a computation of the stratified turbulent flow-field near the Lockheed baseline Ocean Thermal Power Plant (OTPP) design, with zero ambient current. The calculation uses our two-dimensional near-field computer code NRFL02, and approximates the flow associated with one of the four power modules by assuming a rectangular domain of depth 500 ft, with horizontal slots at one end to represent the warm inflow and the two outflows. We assume that the flow is statistically uniform across the width of this domain. Widths of</p> <p>(continued) on p. 73B</p>			

DD FORM 1 JAN 73 1473

EDITION OF 1 NOV 65 IS OBSOLETE
S/N 0102-LF-014-6601

SECURITY CLASSIFICATION OF THIS PAGE (When Data Entered)

408 404

20. ABSTRACT (continued)

50 ft, 100 ft, 200 ft, and 400 ft are separately assumed; ~~we believe that~~ the 100-ft and 200-ft computations essentially bracket the results for the prototype flow.

The numerical results for the average warm inflow temperatures, in the four cases, are 75.7 F, 77.2 F, 77.9 F, and 78.6 F. This is with a surface temperature of 80 F. The warm outflow is defined to be 3 F cooler; the cold outflow temperature is set to 45 F. (4)

The numerical results for the OTHP-generated turbulent diffusivity indicate that it is effectively confined to the neighborhood of the plant. Its value is very small outside such a neighborhood. ↙

Conclusions are drawn with regard to OTHP operation and modeling.

TABLE OF CONTENTS

	<u>Page</u>
ABSTRACT.	111
1. INTRODUCTION.	1-1
2. NRFLO2 MODEL OF THE LOCKHEED NEAR-FIELD FLOW CONDITIONS .	2-1
2.1 The Lockheed Baseline OTHF Design	
2.2 NRFLO2 Model of the Lockheed Design	
2.3 NRFLO2 Turbulence Model	
2.4 The Assumed Ambient Ocean Conditions	
3. RESULTS AND DISCUSSION.	3-1
3.1 Numerical Results	
3.2 Validity of the Results	
3.3 Conclusions	
ACKNOWLEDGEMENTS.	A-1
REFERENCES.	R-1

ABSTRACT

This report describes a computation of the stratified turbulent flow-field near the Lockheed baseline Ocean Thermal Power Plant (OTPP) design, with zero ambient current. The calculation uses our two-dimensional near-field computer code NRFLO2, and approximates the flow associated with one of the four power modules by assuming a rectangular domain of depth 500 ft, with horizontal slots at one end to represent the warm inflow and the two outflows. We assume that the flow is statistically uniform across the width of this domain. Widths of 50 ft, 100 ft, 200 ft, and 400 ft are separately assumed; we believe that the 100 ft and 200 ft computations essentially bracket the results for the prototype flow.

The numerical results for the average warm inflow temperatures, in the four cases, are 75.7°F , 77.2°F , 77.9°F , and 78.6°F . This is with a surface temperature of 80°F . The warm outflow is defined to be 3°F cooler; the cold outflow temperature is set to 45°F .

The numerical results for the OTTP-generated turbulent diffusivity indicate that it is effectively confined to the neighborhood of the plant. Its value is very small outside such a neighborhood.

Conclusions are drawn with regard to OTTP operation and modeling.

1. INTRODUCTION

We have discussed the external flow problems associated with ocean thermal power plant (OTPP) operation in previous reports (Piacsek, Toomre, and Roberts, 1975, and Piacsek, Martin, Toomre, and Roberts, 1976). The first problem concerns the warm and cold OTPP inflows. With a poor design, there is strong turbulent mixing and recirculation of outflow water, resulting in a substantial reduction in the temperature difference constituting the thermal resource. The second problem concerns the environmental impact of OTPP operation; large-scale implementation in limited ocean regions may produce significant thermal and other changes, either beneficial or otherwise.

Our computer code NRFL02 for calculating the near-field turbulent flow and the associated temperature distribution is described in Parts I and III of this report series. The first objective of these external flow computations is the determination of the OTPP inflow temperatures, as modified by turbulent mixing and recirculation of outflow water. The second objective is to obtain results which can be used in determining the far-field environmental impact of OTPP operation.

NRFL02 considers a rectangular two-dimensional domain, with outflows and inflows on the left vertical boundary to model the OTPP intakes and outflows. The surface and bottom boundaries are impermeable, while the passive boundary conditions at the right allow horizontal inflow from and outflow to the ambient ocean. A first-order turbulence closure model is used, with a turbulent kinetic energy equation having generation, decay, advection, and diffusion terms. This kinetic energy is used with an imposed length-scale and the local density stratification to calculate the single turbulent diffusivity coefficient, which is used in the equations for the horizontal motion, the vertical motion, the temperature, and the turbulent kinetic energy. Where the horizontal flow is into the computational domain, either on the left (OTPP) boundary or on the

right boundary with the ambient ocean, boundary values of all variables are required. When the flow is out of the computational domain, passive boundary conditions on the normal derivatives are required for the vertical motion, the temperature, and the turbulent kinetic energy.

In this report, we describe the application of NRFL02 to the baseline OTPP design described by Lockheed (Trimble, 1975). This design is probably more amenable to two-dimensional external flow computation than the others described to date. In a sense, this can be regarded as our baseline near-field study; in Part I, we applied NRFL02 to a proposed two-dimensional laboratory simulation of stratified turbulence driven by inflows and outflows.

NRFL02 is the first in a proposed series of near-field computer codes, with increasingly complicated and flexible geometries, OTPP specifications, and numerical methods. We hope to finalize the turbulence closure model in the next code, NRFL0A (with an axisymmetric geometry). The coefficients will be tuned to give agreement with experimental results obtained by other ERDA contractors. Three-dimensional flow fields will then be studied using the code NRFL03.

In Section 2, we describe our model of the Lockheed baseline design and of the ambient ocean, within the constraints of NRFL02. The spar design has an axisymmetric cold water pipe and intake structure, with four power modules symmetrically placed around it. We model the flow for a single module (in a 90° quadrant, with the module at the center) in our two-dimensional code by assuming a three-dimensional rectangular region, with uniform conditions across a fixed width w to represent the azimuthal coordinate. Our left boundary is at a radius of 233 ft from the OTPP axis, and we separately compute w values of 50, 100, 200, and 400 ft. The values 50 and 400 are extreme; we believe that the closest approximation is obtained using a w value in the intermediate range. We model only the upper 500 ft of the ocean, so that the deep cold inflow is excluded from these computations.

Our numerical results are presented and discussed in Section 3, and conclusions are drawn with regard to the Lockheed design. The results are presented using computer graphics and comparison tables. Even for the smallest w value considered, the loss in warm inflow temperature through turbulent mixing and outflow recirculation is only about 3°F . This loss would be significant, but not disastrous to OTHF operation.

2. NRFL02 MODEL OF THE LOCKHEED NEAR-FIELD FLOW CONDITIONS.

2.1 THE LOCKHEED BASELINE OTPP DESIGN.

The Lockheed design is described, in a slightly simplified form, in Figure 2.1 and in the associated caption. In the spar design, a cylindrical body 445 ft high, with a diameter of 200 ft, extends downward from 100 ft below the surface. The cold water pipe is a vertical cylinder 1000 ft long, with outside diameter decreasing from 129 ft to 105 ft, attached at the bottom. The superstructure is a vertical cylinder 180 ft long, with diameter 60 ft, attached to the top, and extending 80 ft above the surface. The warm inflow is a 45° cone, with bottom diameter 170 ft and height 55 ft, extending up from the cylindrical OTPP body and meeting the superstructure cylinder at a depth of 45 ft.

Four power modules are symmetrically placed around the central spar. Each module consists of an evaporator cylinder, of diameter 72 ft and length 133 ft, with a horizontal axis at depth 150 ft, and a similar condenser cylinder, at depth 315 ft, canted downward at 10° at the outflow end. Joining these cylinders is a vertical cylinder containing the turbines and generators and auxiliary equipment. Crew access is provided through a thin horizontal cylinder connection to the plant body. The warm evaporator flow of 12000 cu ft/sec enters from the plant body and flows out horizontally after being cooled by 3°F (Lockheed state a slightly lower figure). The cold condenser flow of 15000 ft³/sec is warmed by about 2.4°F and flows out with a direction 10° below the vertical. The two outflows, for each model, are at a horizontal distance of 233 ft from the OTPP axis, and at depths of 150 ft and 315 ft.

FIGURE 2.1. The Lockheed Baseline OTPP Design

This is a side view, with all dimensions in feet; a top view is shown in Figure 2.2. Four power modules are symmetrically placed around the plant body, a vertical cylinder. The warm inflow of 48000 cu ft/sec enters through the conical superstructure around the plant body, is slightly cooled in the four evaporators, and exists horizontally at depth 150 ft. The cold inflow of 60000 cu ft/sec enters the cold water pipe at a depth of 1545 ft, is slightly warmed in the four condensers, and exits at a depth of 315 ft, directed 10° below the vertical. The evaporators and condensers and the outflow ports all have diameter 72 ft.

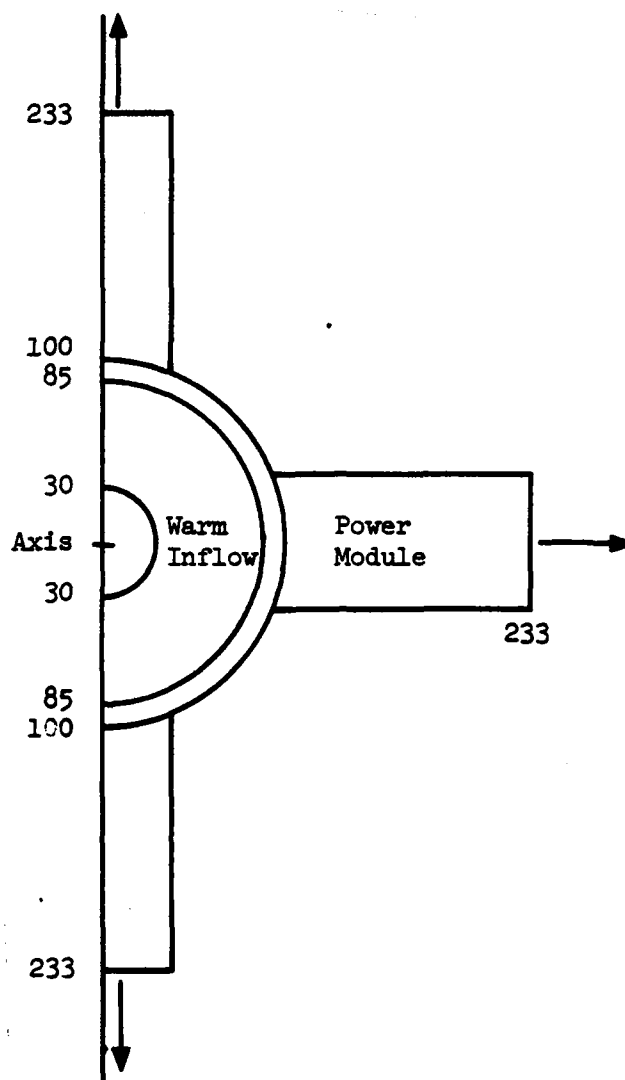


FIGURE 2.2. Top View of the Lockheed Baseline OTHP Design.

A side view is shown in Figure 2.1. All dimensions are in feet. The four power models are attached to a central cylinder of diameter 200 ft. The warm inflow filter is a segment of a 45° cone, with bottom diameter 170 ft, meeting the superstructure cylinder, with diameter 60 ft, at a depth of 45 ft.

The above description is only slightly simplified. We have omitted buoyancy tanks on the side of the main plant body, between the power modules. Similarly we have omitted from the description the buoyancy tanks on the top and bottom of each power module. Otherwise the description is essentially complete.

2.2 NRFL02 MODEL OF THE LOCKHEED DESIGN.

As described in Part I, NRFL02 assumes a rectangular domain, with statistical uniformity across a constant width in the horizontal direction "into the paper". Thus the calculation is two-dimensional. The normal flow distribution is imposed on the left boundary, and is either zero, or into the region (representing an OTPF outflow), or out of the region (representing an OTPF inflow). For outflows, the temperature, vertical motion, and turbulence intensity are also imposed, to complete the modeling of any particular OTPF design.

Thus, to model the Lockheed design, we must first assume a width over which the flow is statistically averaged. The mean flow variables are assumed to be uniform over this width. We have confined attention to the external flow for a single module of the Lockheed design, and to its surface inflow and two outflows. Thus, the inflow flux is 12000 cfs, and the outflow fluxes are 12000 cfs and 15000 cfs. We have modeled these inflows and outflows as occurring through horizontal slots on the left boundary of our computational domain, centered at depths 75 ft, 150 ft, and 315 ft, each slot having a total height of 72 ft. We have made four different assumptions for the width, respectively 50 ft, 100 ft, 200 ft, and 400 ft. These widths should be contrasted with the outflow diameters of 72 ft, and with the dimensions of the inflow cone.

The four widths, and the three horizontal slits, are shown in Figures 2.3 and 2.4, which are otherwise identical to Figures 2.1 and 2.2. The assumption is clearly a gross one. Physically the warm inflow may be expected to be roughly axisymmetric in the surface layers around the cone. The outflow jets should entrain fluid from the sides (Figure 2.4) and from above and below (Figure 2.3). The model includes the vertical entrainment, but the horizontal entrainment is lost in the azimuthal and statistical averaging. Thus, the results can only be regarded as order of magnitude estimates for the near flow.

As the figures show, the 50 ft width assumption gives an outflow area smaller than the prototype circle (3600 sq. ft. as compared with 4071.5 sq. ft.). In addition, the horizontal spreading and entrainment are not at all accurately modeled. We regard this width as too small. Similarly, the assumption of a width of 400 ft is extremely high. The quarter-circumference of a circle with radius 233 ft is only 366 ft. Thus, if the four outflows were combined into a circular slot of height 72 ft, the flow would still be stronger than in the 400 ft model. We believe that the prototype flow is in a sense bracketed by the results obtained assuming widths of 100 ft and 200 ft.

The vertical velocity profiles for the plant inflow and outflows are defined by equations (14) and (15) in Part I. The function $(1 - x^2)^2$ was adopted to avoid the need to resolve discontinuities; the use of a "top-hat" function, or the function $(1 - x^2)^{1/2}$ (to represent the horizontal average over a circular port), might have been more appropriate. Again, this is an approximation, and only order-of-magnitude accuracy can be expected. With a fixed total flux at each port, the choice of this function does not affect the results strongly.

FIGURE 2.3. NRFL02 Model of the
Lockheed Baseline OTHP Design

This figure is a repetition of Figure 2.1, with lines added to indicate the horizontal slots used to model the external flow for a single power module in a rectangular domain. The half-module facing the reader is the one modeled. The warm inflow is modeled by a slot of height 72 ft centered at 75 ft. The warm and cold outflows are modeled by slots of height 72 ft, centered at 150 ft and 315 ft respectively. Four alternative widths for the slots and the computational domain are used, with the half-widths indicated in the figure as 25 ft, 50 ft, 100 ft, and 200 ft. The depth of the computational domain is 500 ft. The left boundary in the figure is a symmetry boundary. Figure 2.4 is a top view of the same computational domain. For each assumed width, the flow speeds are adjusted to give the correct total flux at the inflow and at each outflow.

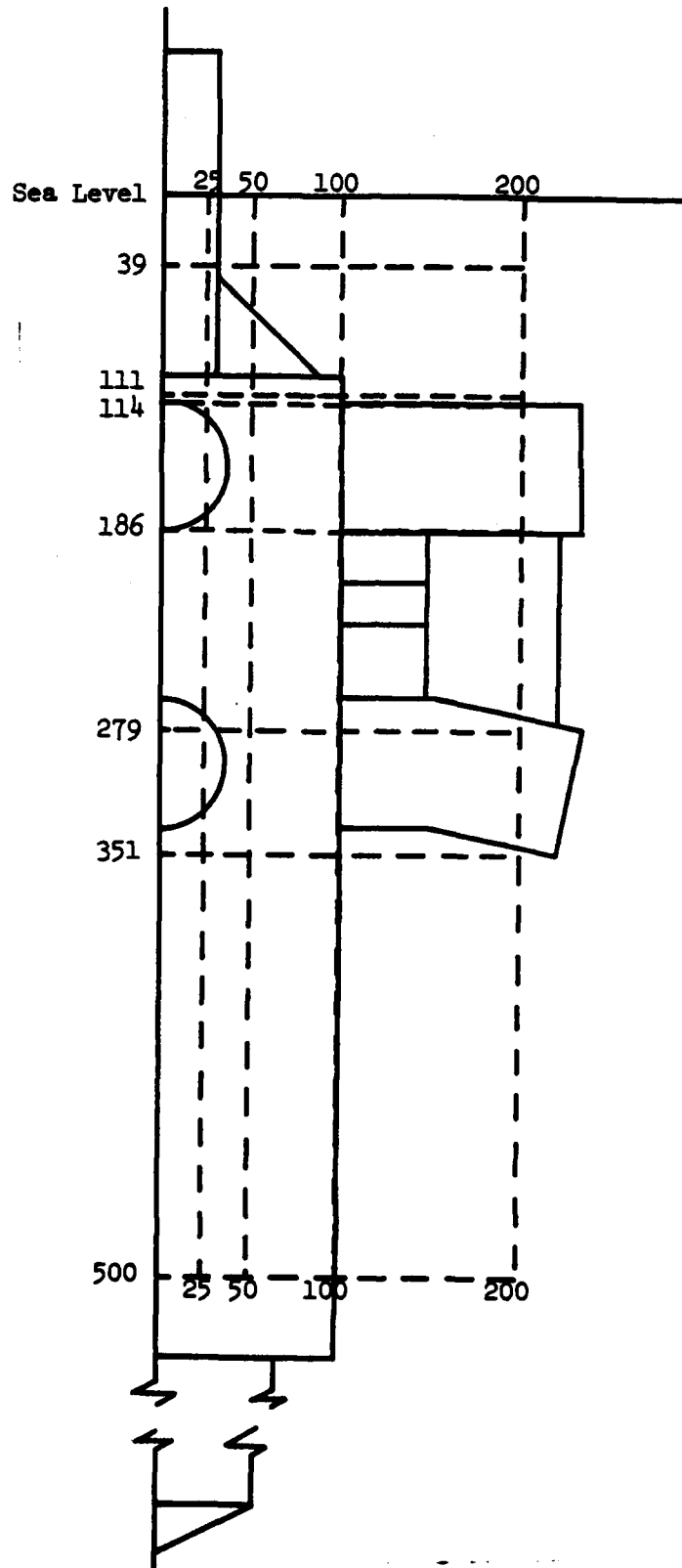
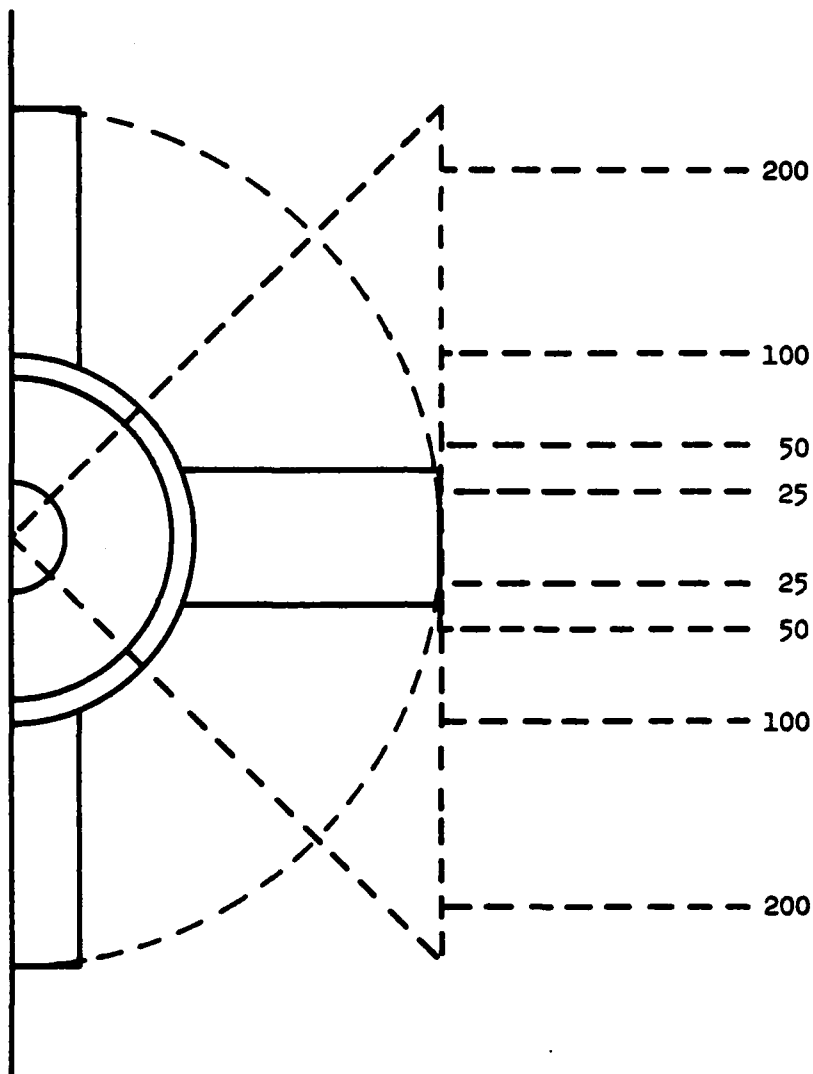


FIGURE 2.3.



**FIGURE 2.4. Top View of the Lockheed Baseline OTHP Design
Showing the Four Alternative Widths for the NRFL02 Model
of the Outflows and Warm Inflow for One Module.**

The rectangular computational domain extends to the right of the power module with depth 500 ft and with the four alternative half-widths shown. The warm inflow segment and the two outflows, are modeled by rectangular ports on the left-hand boundary, occupying the whole width, and with vertical profiles as indicated in Figures 2.3 and 3.9 through 3.12.

The NRFLO2 model of the Lockheed OTPP requires the specification of the temperature, the downward velocity, and the turbulent kinetic energy density, at the outflow ports. These quantities are determined by equations (16) in Part I. The inflow velocity is 10° below the horizontal for the cold inflow. The warm outflow temperature is 3°F colder than the mean warm inflow temperature. The cold outflow is at 45°F , 2.4°F warmer than an assumed cold inflow temperature of 42.6°F in the deep water. The turbulent kinetic energy density is 0.3 times the square of the maximum inflow speed at the port.

2.3 THE NRFLO2 TURBULENCE MODEL

The turbulence model used in NRFLO2 is described in detail in Part I of this report. Briefly, it is a four-parameter first-order statistical closure model, with an imposed length scale, and a single scalar turbulent diffusivity. The turbulent kinetic energy density equation is standard, with generation, decay, advection, and diffusion. The diffusivity determination includes the suppression of vertical turbulent mixing by the density stratification. An added term in the vertical equation of motion represents the damping of vertical motion by turbulence and the coupling with the random internal wave field.

The four parameters used in these computations were chosen on the basis of stratified turbulent wake computations, and have not been tuned to experiments on flows driven by inflows and outflow jets. The values were

$$L = 20 \text{ ft,}$$

$$c_f = 0.5,$$

$$c_s = 0.1,$$

$$c_v = 1.0.$$

The results show a somewhat limited sensitivity to these parameters, because the central effect is that the turbulent kinetic energy, and therefore also the diffusivity, grow for strong shear and decay for strong stratification. The relevant ratio is the Richardson number

$$Ri = N^2 / \frac{1}{2} (u_{i,j} + u_{j,i})^2 .$$

cf. equation (13d) in Part I.

2.4. THE ASSUMED AMBIENT OCEAN CONDITIONS

The code NRFLO2 requires ambient profiles for the temperature and the turbulent kinetic energy density, as described in Parts I and III. The ambient temperature profile is given by equation (18a) of Part I, with

$$T_t = 61.5^\circ\text{F},$$

$$T_r = 14.0^\circ\text{F},$$

$$d_t = 300 \text{ ft},$$

$$z_t = 75 \text{ ft};$$

the profile is displayed in Figures 3.9 through 3.12. The surface temperature is 80°F , the temperature at 500 ft is 44.5°F , and the temperature at very great depths is 39.5°F .

The ambient turbulent kinetic energy density profile is given by equation (18c), with

$$z_E = 125 \text{ ft},$$

$$E_o = 7.4 \times 10^{-8} \text{ ft}^2/\text{sec}^2 .$$

The results are insensitive to the ambient turbulence, provided it is not unreasonably large.

The code NRFL02 assumes zero ambient current. Calculation of the near-field flow for an operating OTHP in the presence of an ambient relative current distribution requires a three-dimensional code. We plan to develop such a code, NRFL03, in the future.

3. RESULTS AND DISCUSSION

3.1. NUMERICAL RESULTS

Our numerical results for the four models of the near-field turbulent flow for the Lockheed baseline OTPP are displayed in three figures for each case and in an accompanying table. The first group of four figures is a blow-up of the stream lines in the left half of the computational domain, together with a listing of the run data, and the result for the mean temperature of the warm inflow. The second group of four figures shows the isotherms and the stream lines for the full computational domain. The third group of four figures shows for each case the contours of the turbulent diffusivity, and the profiles at the left and right boundaries of the temperature and the horizontal motion.

The results for the four assumed region widths are summarized in Table 3.1. The table lists the maximum imposed speeds at the inflow and outflows; these are inversely proportional to the width. The assumed flow profiles are defined using the function $(1 - x^2)^2$, as described in Part I.

The warm inflow temperatures are probably our most important result. The extreme values, for widths 50 ft and 400 ft, are 75.7°F and 78.6°F. We believe that with the assumed ocean temperature profile, the OTPP baseline design would experience an average inflow temperature between 77.2°F and 77.9°F; these are the results for widths 100 ft and 200 ft.

The table also displays the warm outflow temperatures, 3°F cooler than the inflow temperatures. The cold outflow temperatures are imposed, at 45°F; this is 2.4°F warmer than the assumed cold inflow temperature of 42.6°F from the deep water.

FIGURE 3.1 Stream Lines near the
Plant for Width 50 Feet

The displayed domain is 500 ft deep and extends 375 ft to the right of the OTPP outflows; this is the left half of the full computational domain. The outflows are centered at depths 150 ft and 315 ft, with widths 72 ft. The stream lines are drawn at contour intervals of 2000 cu ft/sec. The flux of 15000 cu ft/sec leaving the cold outflow (lines 1 through 7) falls till it finds its own level. In doing so, it entrains 8000 cu ft/sec from the warm outflow (lines 8 through 1). The remaining 4000 cu ft/sec of warm outflow recirculates into the warm inflow (lines 2 and 3). The other 8000 cu ft/sec of warm inflow comes from the surface layers (lines 1, 0, 9 and 8). As a result of turbulent mixing and recirculation, in this very strong flow computation, the mean plant inflow temperature is 75.7°F.

The table at the bottom shows the data used for this computation. This data is dimensionless, and is determined from the dimensional data as described in Part III of this report.

FIGURE 3.2. Stream Lines near the
Plant for Width 100 Feet

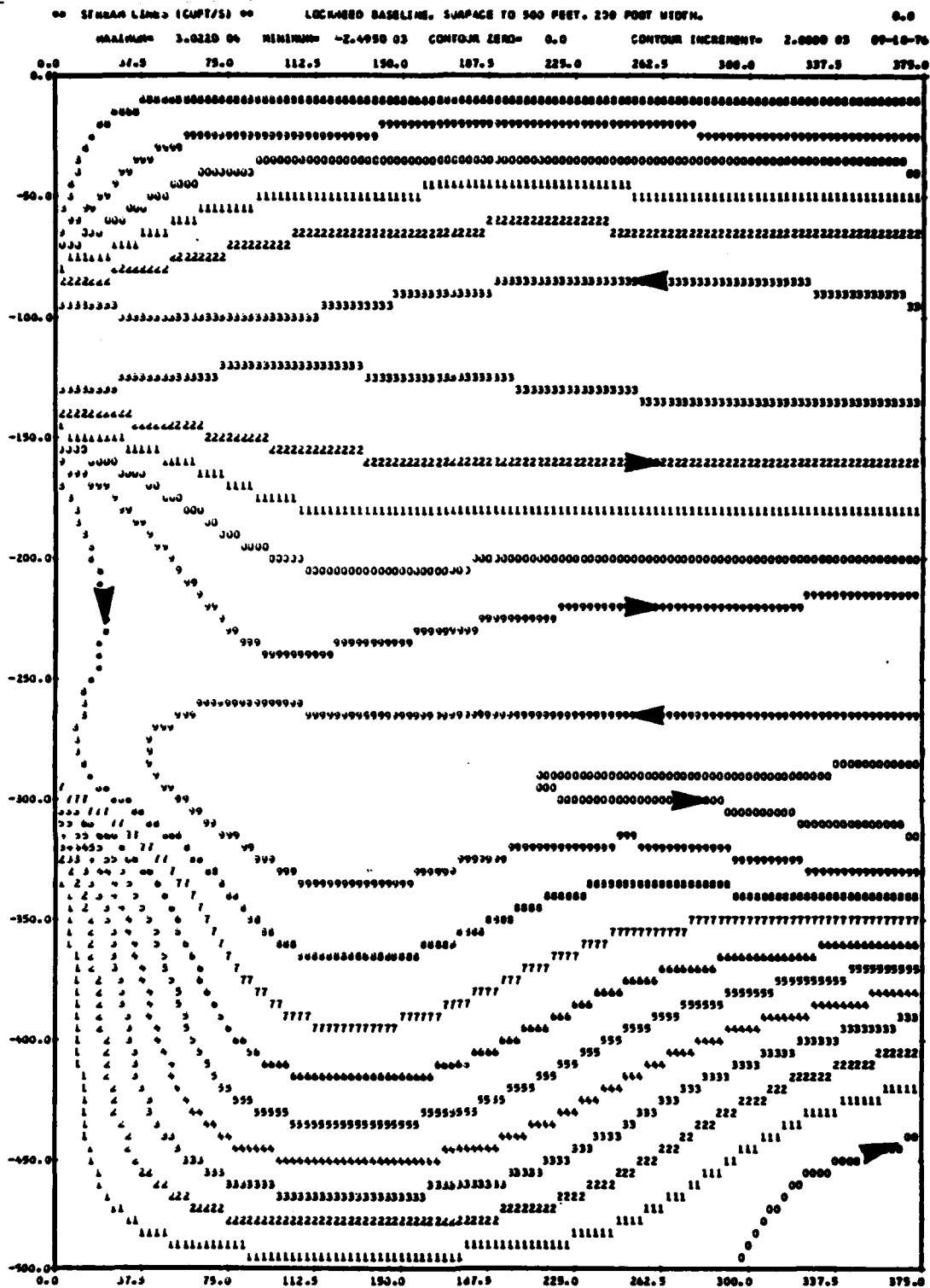
The displayed domain is 500 ft deep and extends 375 ft to the right of the OTHP outflows; this is the left half of the full computational domain. The outflows are centered at depths 150 ft and 315 ft, with widths 72 ft. The stream lines are drawn at contour intervals of 2000 cu ft/sec. The flux of 15000 cu ft/sec leaving the cold outflow (lines 1 through 7) falls till it finds its own level. In doing so, it merges with and entrains 10700 cu ft/sec from the warm outflow (lines 8 through 2). The remaining 1300 cu ft/sec of warm outflow recirculates into the warm inflow (line 3). The remaining 10700 cu ft/sec of warm inflow comes from the surface layers (lines 2 down to 8). As a result of the turbulent mixing and recirculation, in this strong flow computation, the mean plant inflow temperature is 77.2°F.

The table at the bottom shows the data used for this computation. This data is dimensionless, and is determined from the dimensional data as described in Part III of this report.

FIGURE 3.3. Stream Lines near the
Plant for Width 200 Feet

The displayed domain is 500 ft deep and extends 375 ft to the right of the OTPF outflows; this is the left half of the full computational domain. The outflows are centered at depths 150 ft and 315 ft, with widths 72 ft. The stream lines are drawn at contour intervals of 2000 cu ft/sec. The flux of 15000 cu ft/sec (lines 1 through 7) leaving the cold outflow falls past its own level, and rises again. In doing so, it entrains 2000 cu ft/sec from the warm outflow (line 8) and 4000 cu ft/sec from larger distances (lines 9 through 0, coming in at depth 275 ft and leaving at 300 ft). The rest of the warm outflow (lines 9 and 0 through 3) flows out horizontally, except that 300 cu ft/sec recirculate into the warm inflow. The rest of the warm inflow comes in horizontally. As a result of the weak recirculation, and the turbulent heat transport, the mean inflow temperature is 77.9°F.

The table at the bottom shows the data used for this computation. This data is dimensionless, and is determined from the dimensional data as described in Part III of this report.



LOCATED BASELINE, SURFACE TO 500 FEET, 200 FOOT WIDTH.
 HARM PLANT INFLUX AT 75 FEET, WITH SAME RADIUS AS OUTFLOW.
 JUTPLND TEMPERATURE IS 2 DEGREES FAHRENHEIT COLDER THAN
 HARM INFLUX TEMPERATURE.
 CBL PLANT JUTPLND AT 115 FEET, TEMPERATURE 45 FAHRENHEIT.

HARM PLANT INFLUX TEMPERATURE IS 77.9

AMPV	-0.0131	0.0131	0.0103	0.0
AMPQ	0.0	0.300	0.300	0.0
TANALP	3.0	0.0	-0.160	0.0
TPAH	-3.0	70.0	45.0	45.0
WPL	0.072	0.072	0.072	0.072
ZCENT	0.050	0.700	0.370	3.000
FT,FB,ZTC,WED	00.0	44.5	0.400	0.100
JAMB,ODBP		1.00-09	0.25	
PLEN,CP,CS,CU,PORC	0.040	0.300	0.100	1.000
JAP,XSTICH,ISTICH,II,JJ	1.500	1.500	0.0	12 34
TIME,CPL,MDUTPT,USCALC,WIOFT	10.0	0.00	2	900.0 200.0

30-10-76

FIGURE 3.4.

FIGURE 3.4. Stream Lines near the
Plant for Width 400 Feet

The displayed domain is 500 ft deep and extends 375 ft to the right of the OTHP outflows; this is the left half of the full computational domain. The outflows are centered at depths 150 ft and 315 ft, with widths 72 ft. The stream lines are drawn at contour intervals of 3000 cu ft/sec. The flux of 15000 cu ft/sec (lines 1 through 5) leaving the cold outflow falls till it finds its own level. In doing so, it entrains 3000 cu ft/sec of deep cold water (line A) and 10000 cu ft/sec of water from about 280 ft (lines 6 through 8). The warm outflow of 12000 cu ft/sec mostly flows out horizontally (lines 6 through 8), entraining about 1000 cu ft/sec both above and below (lines 5 and 9). The recirculation flux is only 100 cu ft/sec in this weak flow case (line 9). The mean inflow temperature is 78.6°F. There is very little reduction due to recirculation or turbulent heat transport in this weak flow computation.

The table at the bottom shows the data used for this computation. This data is dimensionless, and is determined from the dimensional data as described in Part III of this report.

FIGURE 3.5. Temperature Distribution and
Stream Lines for Width 50 Feet

The displayed domain is 500 ft by 750 ft, and is the whole of the computational domain. The left half of the stream lines figure is shown expanded in Figure 3.1. The temperature contours labeled 6 through 9 and 0 through 6 correspond to multiples from 16 through 26 of the contour increment 3°F , and thus, to temperatures from 48°F to 78°F . The stream lines are drawn at a contour increment of 3000 cu ft/sec, and thus, show 15000 cu ft/sec leaving the cold outflow, and a further 12000 cu ft/sec leaving the warm outflow and entering the warm inflow. The surface is a 15000 cu ft/sec contour, with the label 5.

The isotherms and stream lines are roughly horizontal over most of the region. There are irregularities at the artificial boundary on the right, where the flow is adjusted to find its own density level, and there is evidence of some remaining fluctuations in the form of internal waves. The temperature is not constant on stream lines near the left boundary, because of the turbulent diffusivity distribution shown in Figure 3.9. This effect is pronounced near the warm inflow, where the 78°F contour crosses two stream lines.

The flow pattern shown by the stream lines is discussed in the caption to Figure 3.1.

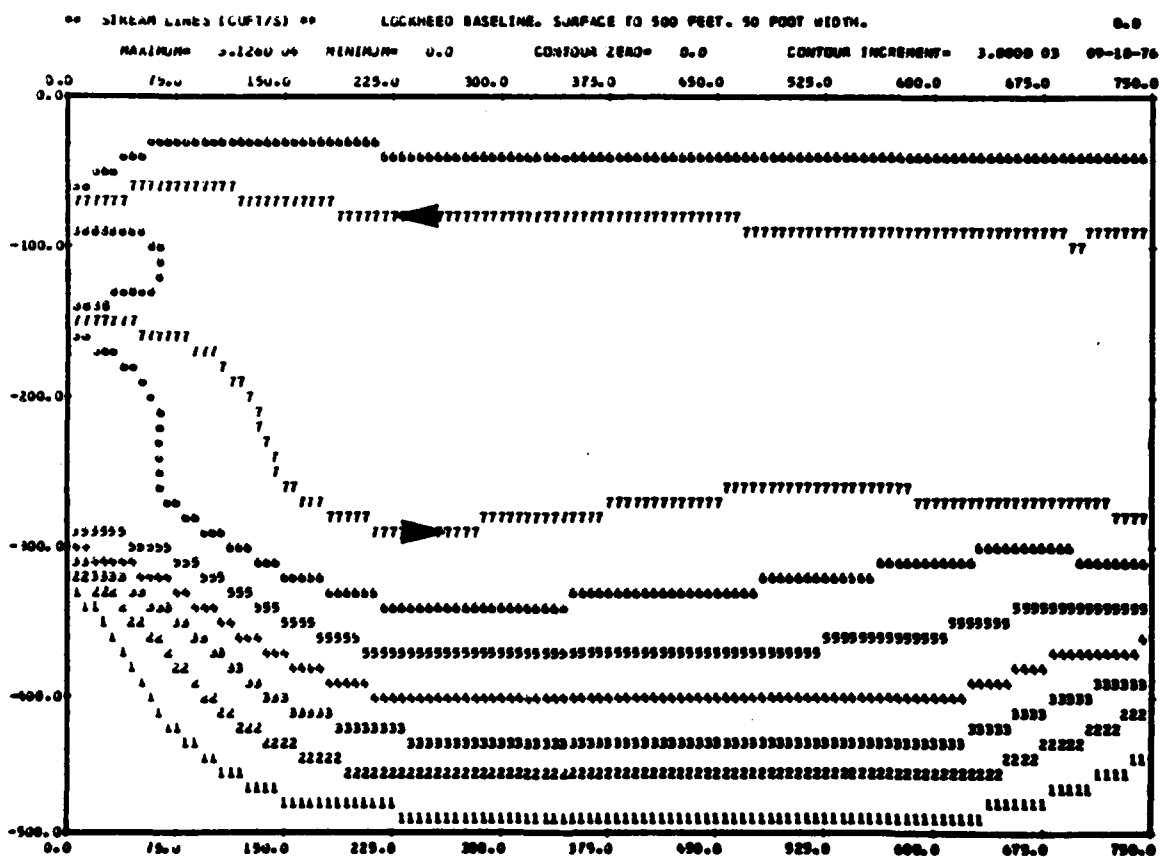
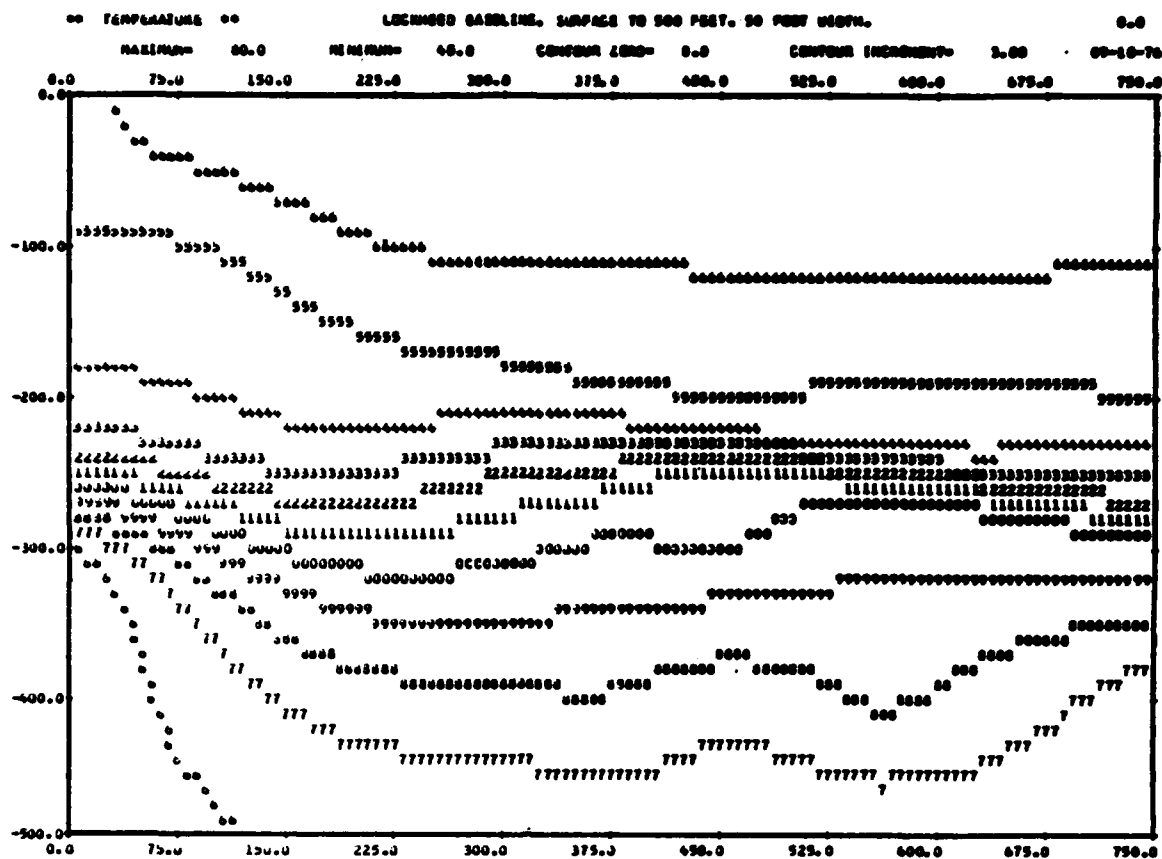


FIGURE 3.5.

FIGURE 3.6. Temperature Distribution and
Stream Lines for Width 100 Feet

The displayed domain is 500 ft by 750 ft, and is the whole of the computational domain. The left half of the stream lines figure is shown expanded in Figure 3.2. The temperature contours labeled 5 through 9 and 0 through 6 correspond to multiples from 15 through 26 of the contour increment 3°F , and thus, to temperatures from 45°F to 78°F . The stream lines are drawn at a contour increment of 3000 cu ft/sec, and thus, show 15000 cu ft/sec leaving the cold outflow, and a further 12000 cu ft/sec leaving the warm outflow and entering the warm inflow. The surface is a 15000 cu ft/sec contour, with the label 5.

The isotherms and stream lines are roughly horizontal over most of the region. There are irregularities at the artificial boundary on the right, where the flow is adjusted to find its own density level, and there is evidence of some remaining fluctuations in the form of internal waves. The temperature is not constant on stream lines near the left boundary, because of the turbulent diffusivity distribution shown in Figure 3.10. Nevertheless, a substantial part of the inflow water is at temperatures over 78°F , and the average inflow temperature is 77.2°F .

The flow pattern shown by the stream lines is discussed in the caption to Figure 3.2.

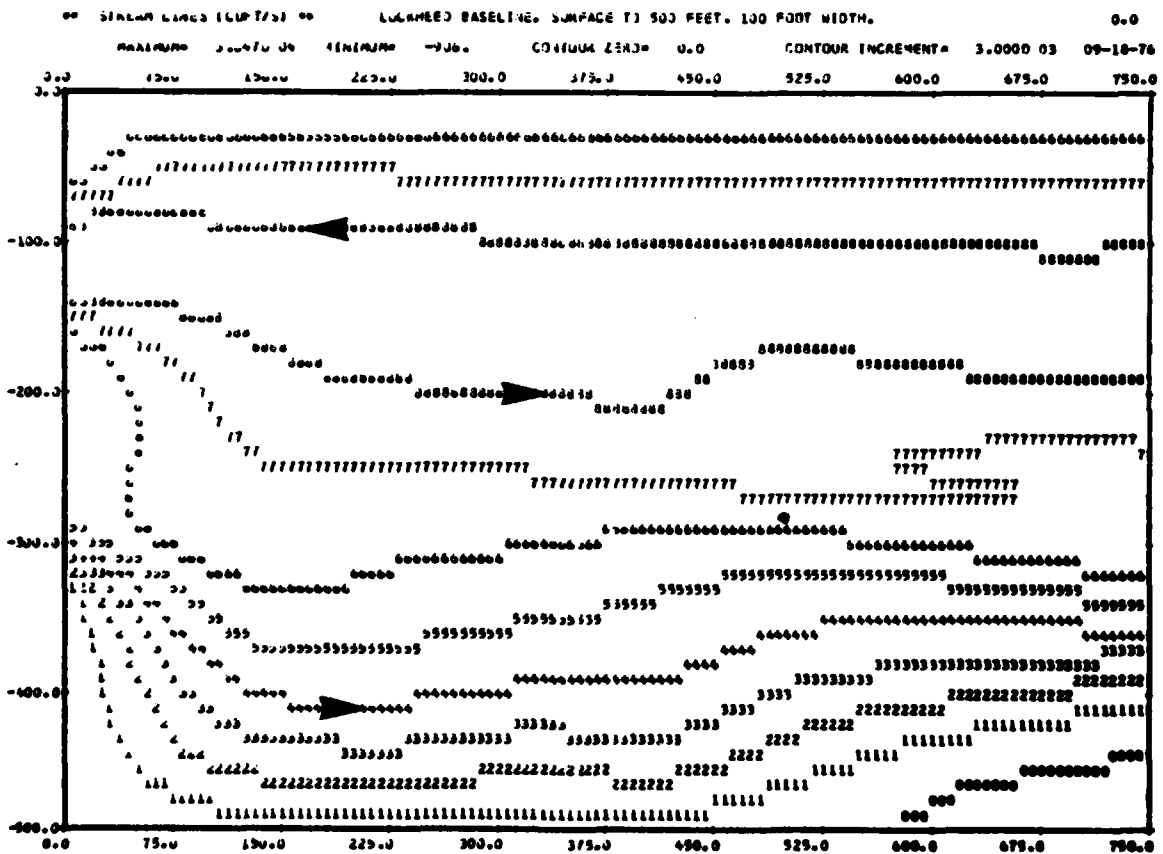
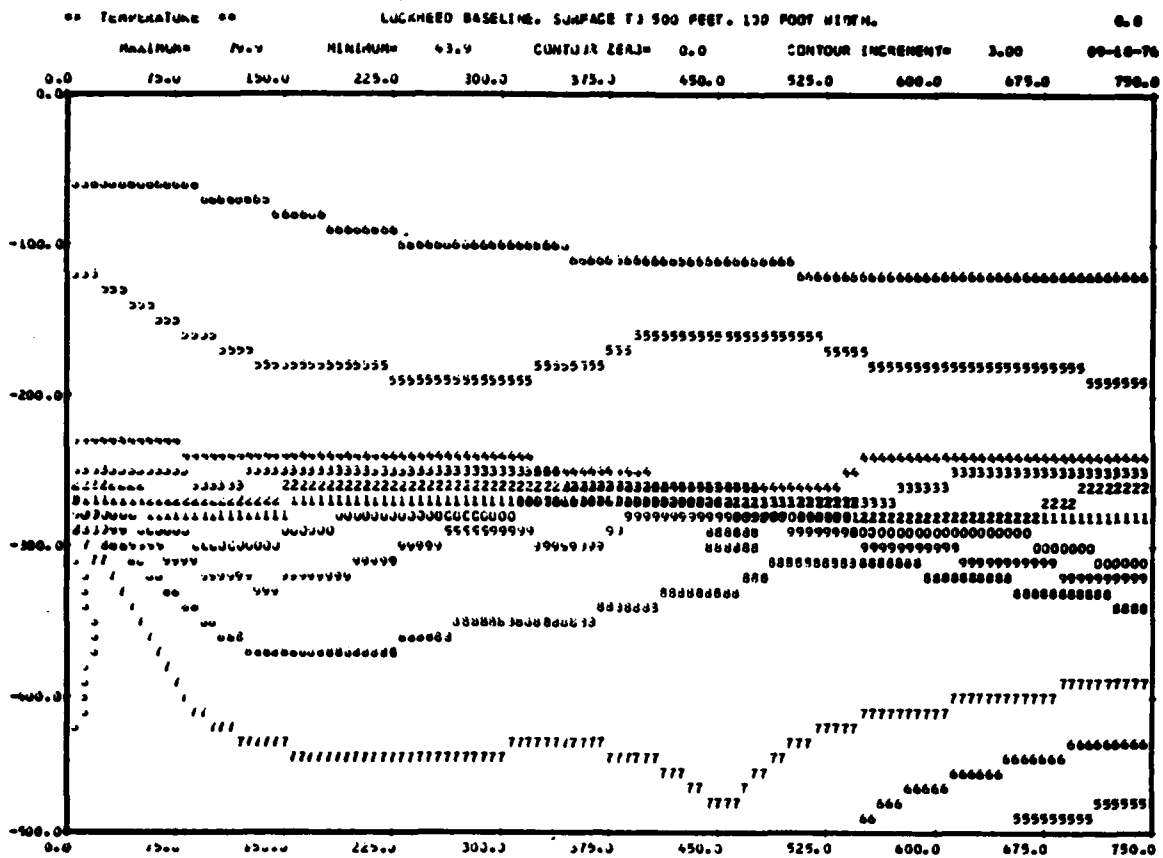


FIGURE 3.6.

**FIGURE 3.7. Temperature Distribution and
Stream Lines for Width 200 Feet**

The displayed domain is 500 ft by 750 ft, and is the whole of the computational domain. The left half of the stream lines figure is shown expanded in Figure 3.3. The temperature contours labeled 5 through 9 and 0 through 6 correspond to multiples from 15 through 26 of the contour increment 3°F , and thus, to temperatures from 45°F to 78°F . The stream lines are drawn at a contour increment of 5000 cu ft/sec, and thus, show 15000 cu ft/sec leaving the cold outflow, and a further 12000 cu ft/sec leaving the warm outflow and entering the warm inflow. The surface is a 15000 cu ft/sec contour, with the label 3.

The isotherms and stream lines are roughly horizontal over most of the region. There are irregularities at the artificial boundary on the right, where the flow is adjusted to find its own density level, and there is evidence of some remaining fluctuations in the form of internal waves. The temperature is not constant on stream lines near the left boundary, because of the turbulent diffusivity distribution shown in Figure 3.11. The 78°F contour reaches the left boundary at 80 ft, and the mean inflow temperature is 77.9°F . A strong thermocline separates the warm outflow from the cold outflow.

The flow details, and the entrainment from infinity, are discussed in the Figure 3.3 caption.

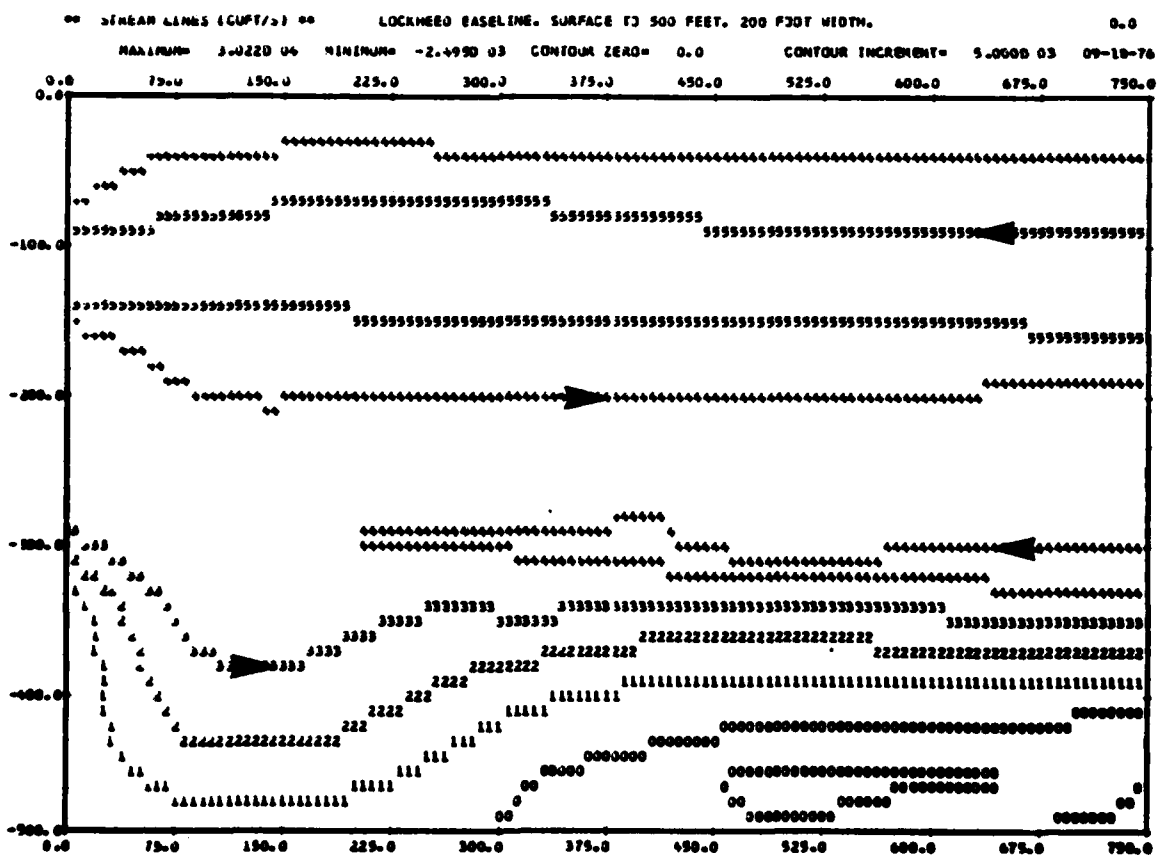
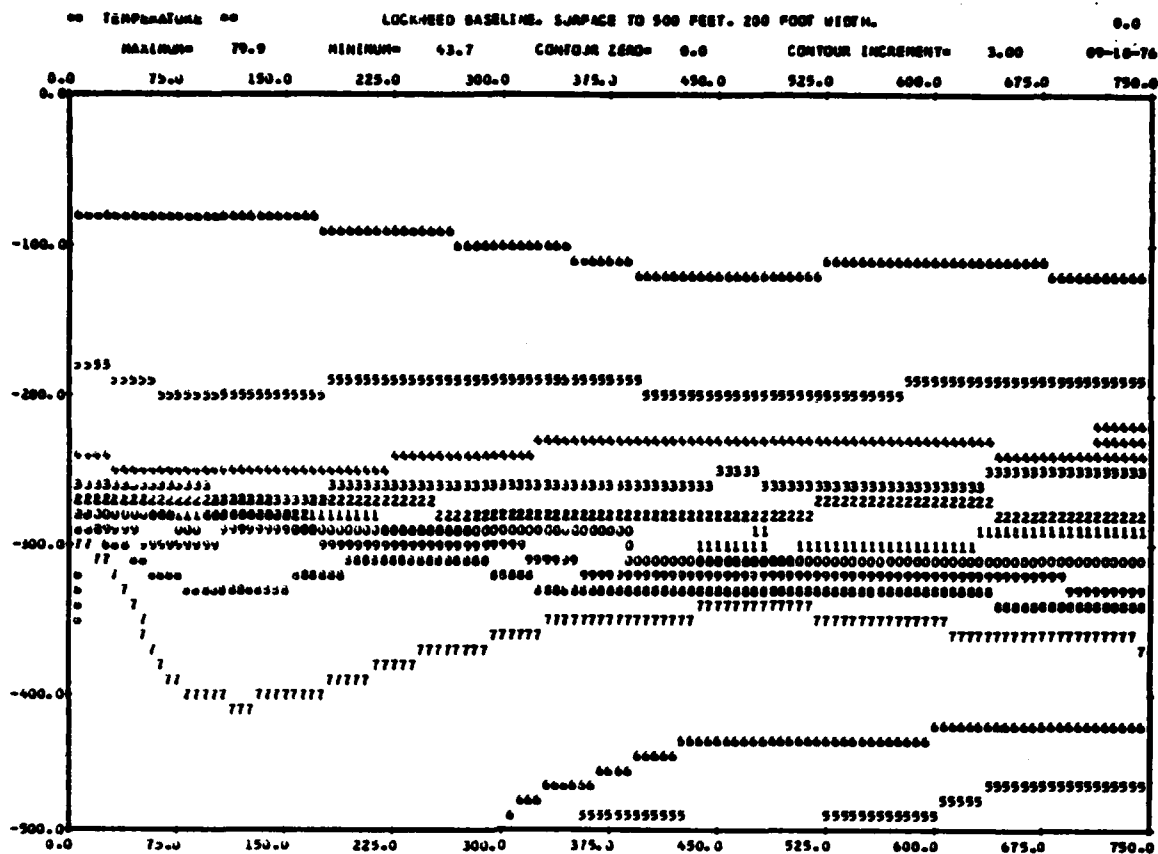


FIGURE 3.7.

FIGURE 3.8. Temperature Distribution and
Stream Lines for Width 400 Feet

The displayed domain is 500 ft by 750 ft, and is the whole of the computational domain. The left half of the stream lines figure is shown expanded in Figure 3.4. The temperature contours labeled 5 through 9 and 0 through 6 correspond to multiples from 15 through 26 of the contour increment 3°F , and thus, to temperatures from 45°F to 78°F . The stream lines are drawn at a contour increment of 5000 cu ft/sec, and thus, show 15000 cu ft/sec leaving the cold outflow, and a further 12000 cu ft/sec leaving the warm outflow and entering the warm inflow. The surface is a 15000 cu ft/sec contour, with the label 3.

The isotherms and stream lines are roughly horizontal over most of the region. There are irregularities at the artificial boundary on the right, where the flow is adjusted to find its own density level, and there is evidence of some remaining fluctuations in the form of internal waves. The temperature is practically constant on stream lines near the left boundary, because of the small turbulent diffusivity distribution shown in Figure 3.12. The 78°F isotherm crosses the left boundary at 90 ft, and the mean inflow temperature is 78.6°F .

The stream lines are discussed in the Figure 3.4 caption. There is substantial entrainment above and below both outflow jets.

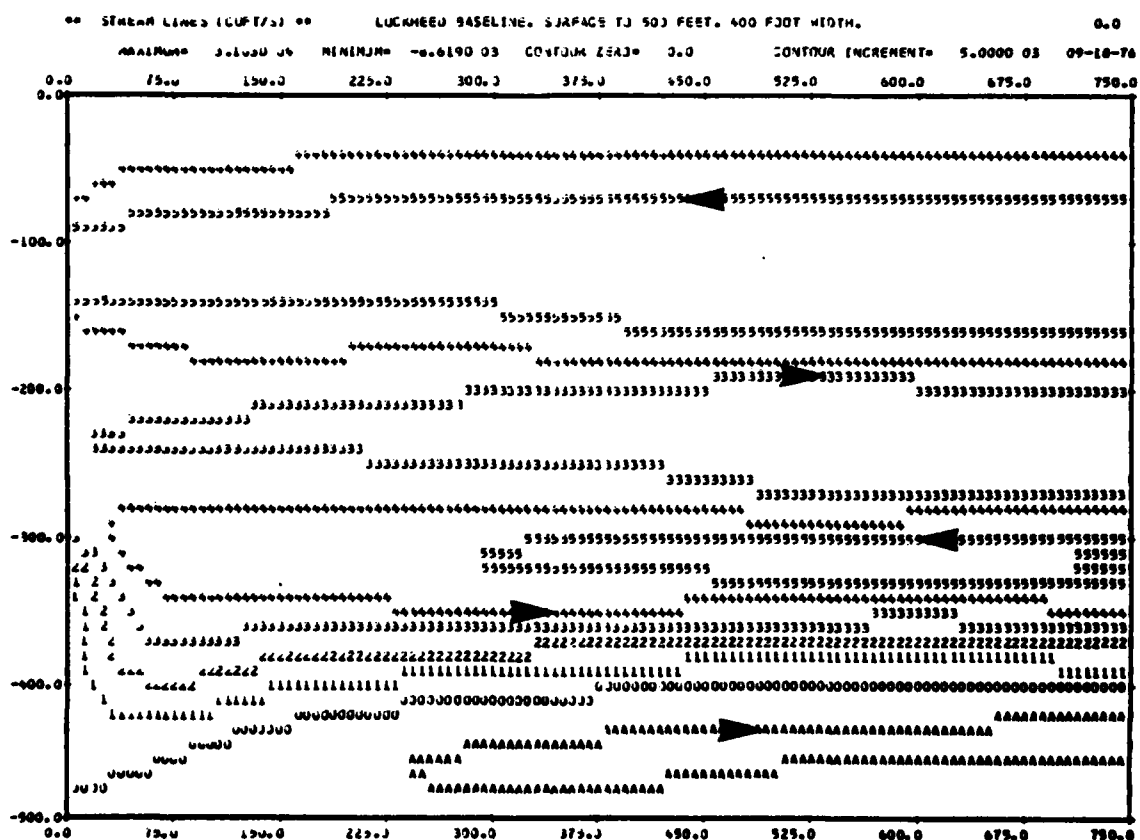
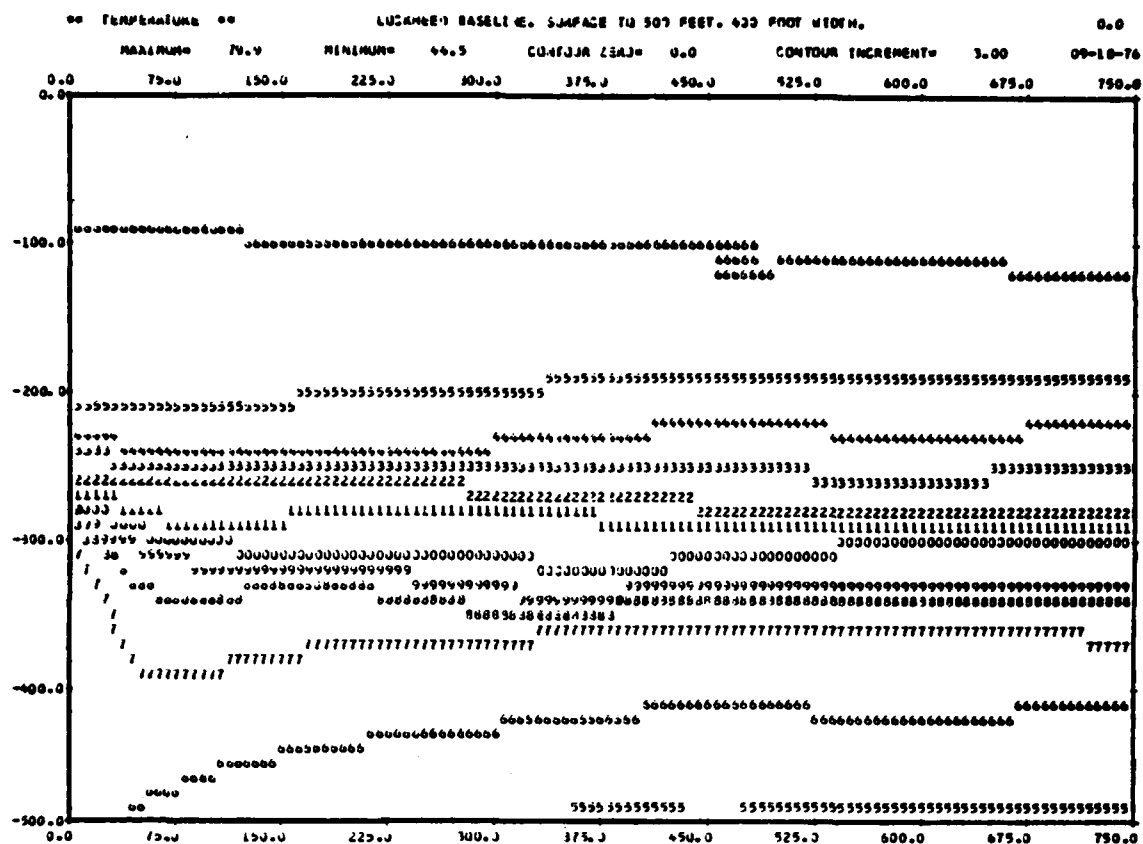


FIGURE 3.8.

FIGURE 3.9. Diffusivity Distribution, and
Boundary Profiles of Horizontal Flow and
Temperature, for Width 50 Feet

The turbulent diffusivity is displayed in a domain 500 ft by 750 ft, with a contour increment of $15 \text{ ft}^2/\text{sec}$. The contour labels are multiples of this increment. The diffusivity reaches its maximum of $85.5 \text{ ft}^2/\text{sec}$ at the cold outflow, and is only slightly smaller at the warm inflow and outflow. The minimum value on the left boundary is $40.1 \text{ ft}^2/\text{sec}$, and it drops rapidly with distance from the plant, at all depths.

In the lower figure the scales for the horizontal flow U and the temperature T and ambient temperature A , are as shown. The ambient temperature increases from 44.5°F to 80°F , as described in Section 2.4. The flow profile on the left boundary is imposed to represent the warm inflow at 75 ft and the warm and cold outflows at 150 ft and 315 ft; the maximum speeds are 6.38 ft/sec, 6.38 ft/sec, and 8.50 ft/sec. The flow profile on the right is towards the plant down to 160 ft; most of this flux eventually enters the warm inflow.

The temperature on the left boundary is 45°F at the cold outflow, and 72.7°F at the warm outflow. This is 3°F cooler than the average inflow temperature. The temperature at the left boundary is substantially below the ambient temperature. The flow is adjusted near the right boundary so that the outflow finds its own density level; this adjustment was successful here except that there was no water to flow out at below 50°F , because of the turbulent mixing.

The horizontal flow in the lower right figure determines the far-field environmental impact. Water is added to the ambient ocean in certain temperature and density ranges, and is withdrawn from the ambient ocean in others. With very large scale OTHF operations, the thermocline structure and current system will be modified.

FIGURE 3.10. Diffusivity Distribution, and
Boundary Profiles of Horizontal Flow and
Temperature, for Width 100 Feet

The turbulent diffusivity is displayed in a domain 500 ft by 750 ft, with a contour increment of $7.5 \text{ ft}^2/\text{sec}$. The contour labels are multiples of this increment. The diffusivity reaches its maximum of $42.9 \text{ ft}^2/\text{sec}$ at the cold outflow, and is only slightly smaller at the warm inflow and outflow. The minimum value on the left boundary is $18.7 \text{ ft}^2/\text{sec}$, and it drops rapidly with distance from the plant, at all depths.

In the lower figure the scales for the horizontal flow U and the temperature T and ambient temperature A , are as shown. The ambient temperature increases from 44.5°F to 80°F , as described in Section 2.4. The flow profile on the left boundary is imposed, to represent warm inflow at 75 ft and the warm and cold outflows at 150 ft and 315 ft; the maximum speeds are 3.19 ft/sec, 3.19 ft/sec, and 4.25 ft/sec. The flow profile on the right is towards the plant down to 150 ft; most of this flux eventually enters the warm inflow, but there is some entrainment by the warm outflow jet leaving at 200 ft. The cold outflow leaves between depths of 300 ft and 450 ft, and there are small inflow regions above and below, due to entrainment.

The temperature on the left boundary is 45°F at the cold outflow and 74.2°F at the warm outflow (3°F cooler than the average of the warm inflow). The temperature on the right agrees well with the ambient temperature distribution.

The horizontal flow in the lower right figure determines the far-field environmental impact. Water is added to the ambient ocean in certain temperature and density ranges, and is withdrawn from the ambient ocean in others. With very large scale OTHF operations, the thermocline structure and current system will be modified.

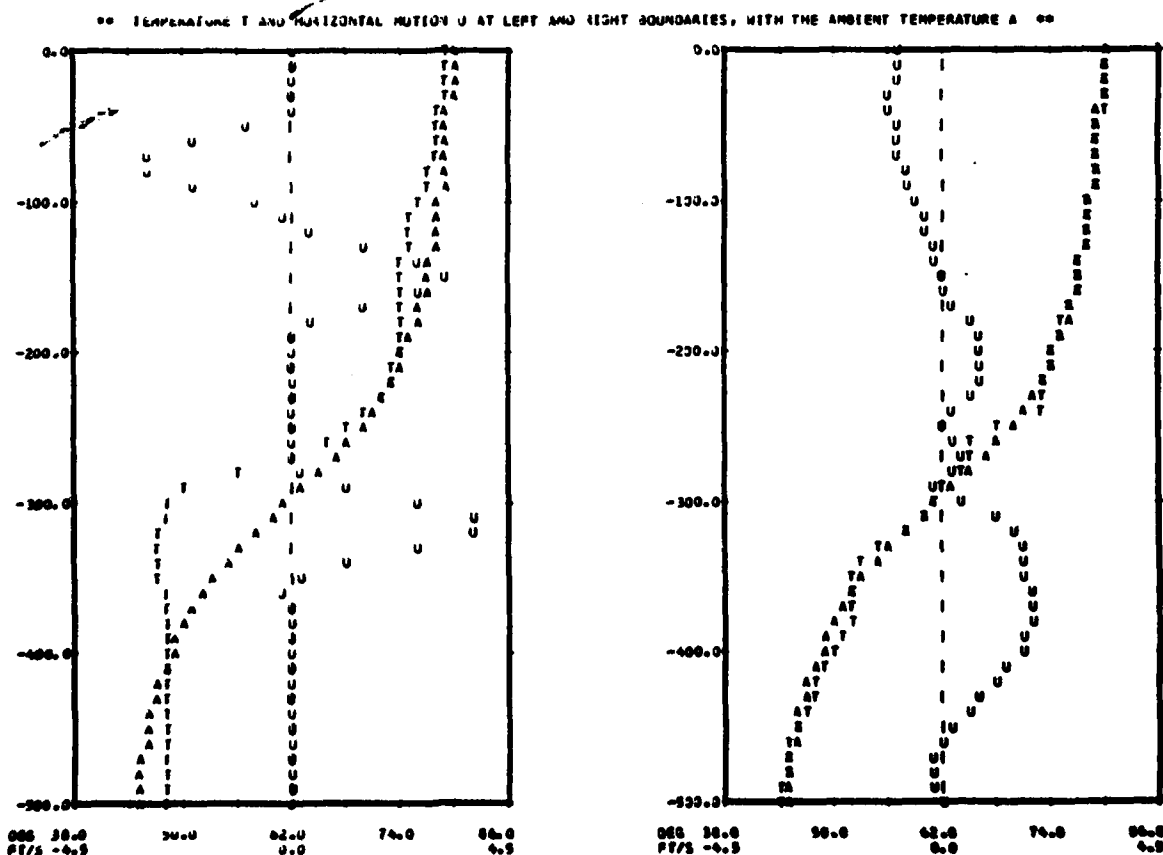
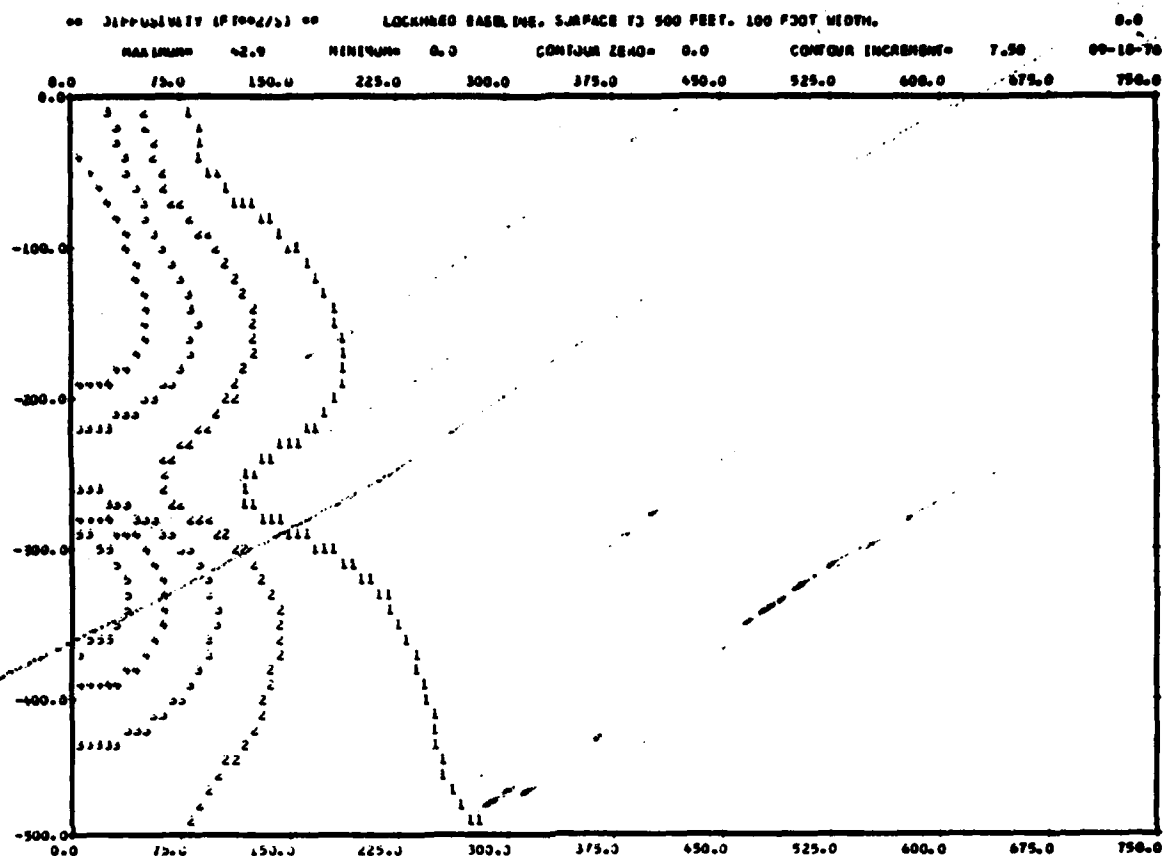


FIGURE 3.10.

FIGURE 3.11. Diffusivity Distribution, and
Boundary Profiles of Horizontal Flow and
Temperature, for Width 200 Feet

The turbulent diffusivity is displayed in a domain 500 ft by 750 ft, with a contour increment of $3 \text{ ft}^2/\text{sec}$. The contour labels represent multiples of this increment. The diffusivity reaches its maximum of $21.7 \text{ ft}^2/\text{sec}$ at the cold inflow, and is only slightly smaller at the warm outflow. The minimum value on the left boundary is $7.1 \text{ ft}^2/\text{sec}$, and it drops rapidly with distance from the plant, at all depths.

In the lower figure the scales for the horizontal flow U and the temperature T and the ambient temperature A , are as shown. The ambient temperature increases from 44.5°F to 80°F , as described in Section 2.4. The flow profile on the left boundary is imposed, to represent the warm inflow at 75 ft and the warm and cold outflows at 150 ft and 315 ft; the maximum speeds are 1.60 ft/sec, 1.60 ft, and 2.12 ft/sec. The flow profile on the right is towards the plant down to 120 ft; some of this flux eventually enters the warm inflow and some is entrained. The warm and cold outflows at 190 ft and 370 ft have inflow regions, above and below, due to entrainment. The flow has been adjusted successfully so that the temperature distribution agrees with the ambient temperature.

The temperature on the left boundary is 45°F and 74.9°F at the outflows. At the inflow the temperature is close to the ambient temperature, with average value 77.9°F .

The horizontal flow in the lower right figure determines the far-field environmental impact. Water is added to the ambient ocean in certain temperature and density ranges, and is withdrawn from the ambient ocean in others. With very large scale OTHF operations, the thermocline structure and current system will be modified.

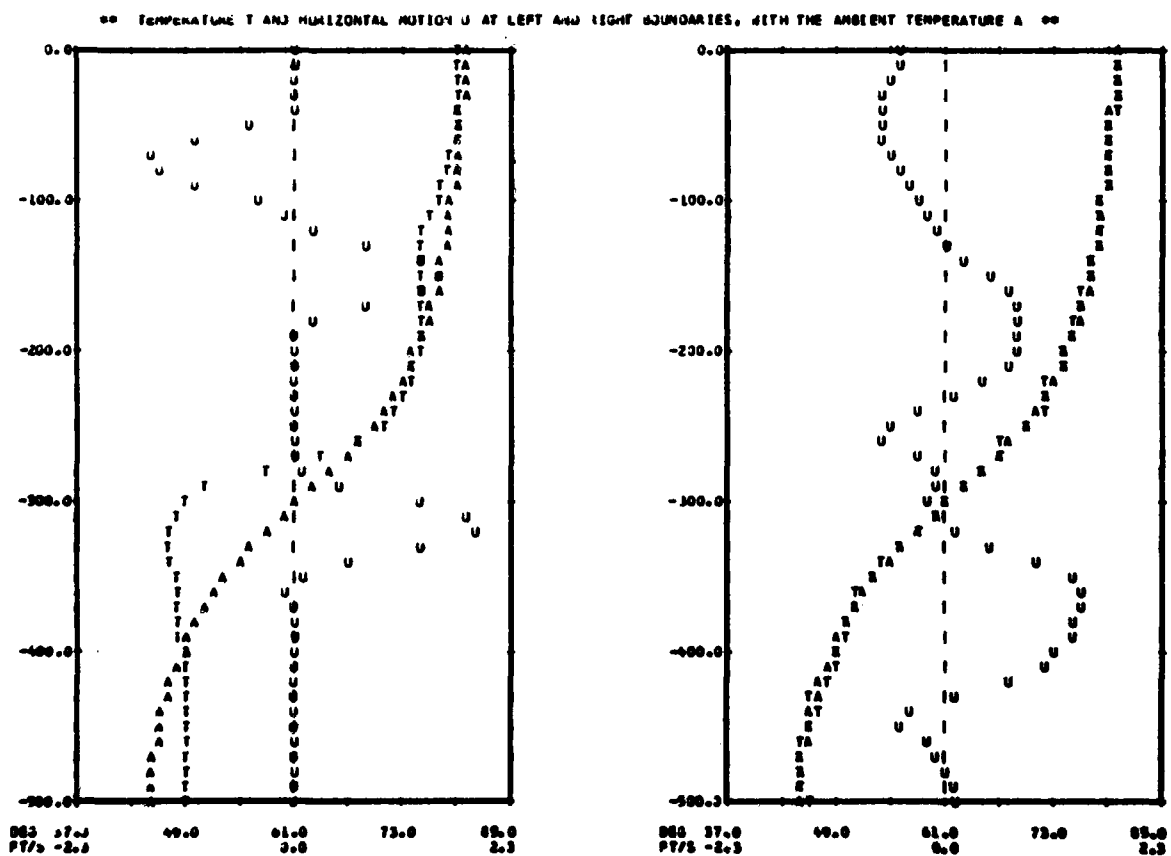
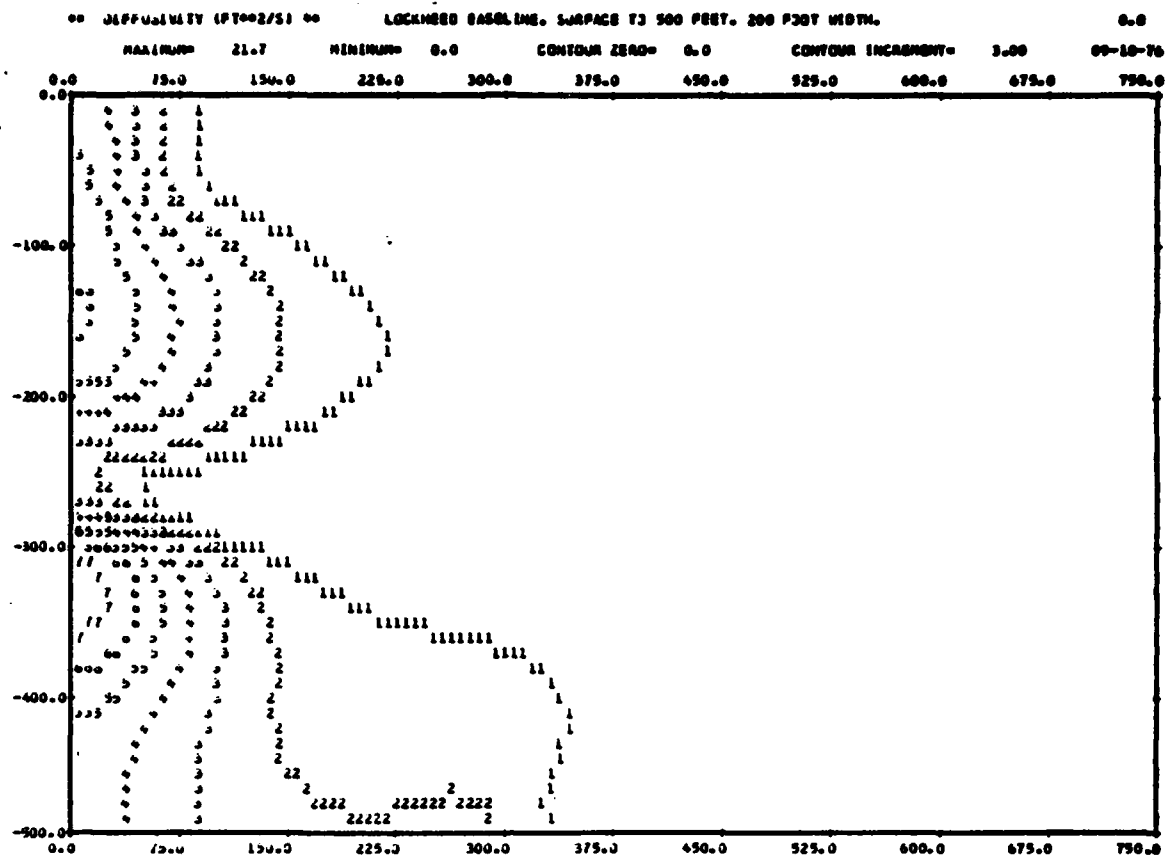


FIGURE 3.11.

FIGURE 3.12. Diffusivity Distribution, and
Boundary Profiles of Horizontal Flow and
Temperature, for Width 400 Feet

The turbulent diffusivity is displayed in a domain 500 ft by 750 ft, with a contour increment of $2 \text{ ft}^2/\text{sec}$. The contour labels represent multiples of this increment. The diffusivity reaches its maximum of $13.5 \text{ ft}^2/\text{sec}$ at the cold outflow, and is only slightly smaller at the warm inflow and outflow. The minimum value on the left boundary is $0.4 \text{ ft}^2/\text{sec}$, and it drops rapidly with distance from the plant, at all depths. Thus, there is effectively no turbulent cooling of the surface layers by the cold outflow.

In the lower figure the scales for the horizontal flow U and the temperature T and ambient temperature A , are as shown. The ambient temperature increases from 44.5°F to 80°F , as described in Section 2.4. The flow profile on the left boundary is imposed, to represent the warm inflow at 75 ft and the warm and cold outflows at 150 ft and 315 ft; the maximum speeds are 0.80 ft/sec, 0.80 ft/sec, and 1.06 ft/sec. The flow profile on the right is complicated; the warm and cold outflow jets, at depths 185 ft and 370 ft, each have inflow regions above and below due to entrainment. The inflow temperature profile on the left is very close to the ambient temperature, and the mean plant inflow temperature is 78.6°F . The warm outflow temperature is 75.6°F (3°F cooler); the cold outflow is at 45°F , (2.4°F warmer than the deep cold inflow).

The horizontal flow in the lower right figure determines the far-field environmental impact. Water is added to the ambient ocean in certain temperature and density ranges, and is withdrawn from the ambient ocean in others. With very large scale OTEP operations, the thermocline structure and current system will be modified.

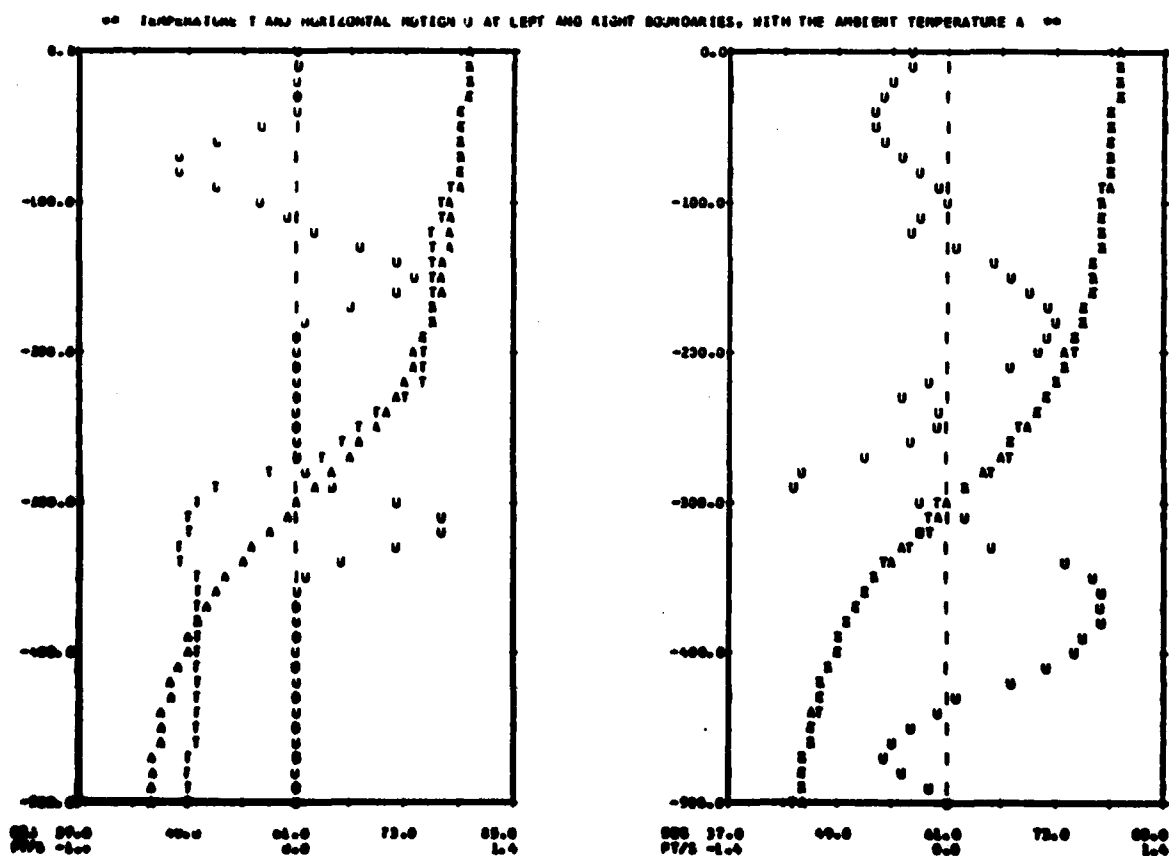
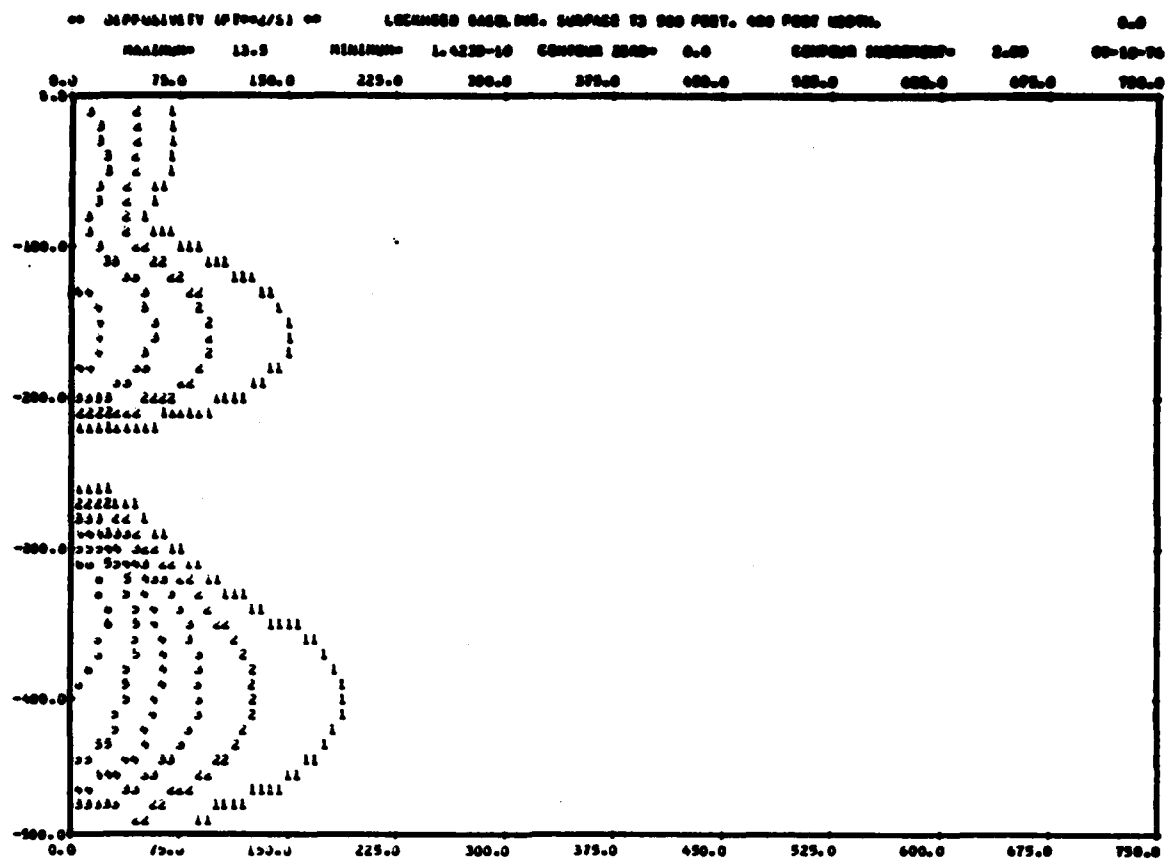


FIGURE 3.12.

TABLE 3.1. Summary of the Numerical Results

QUANTITY	UNIT	VALUES			
		50	100	200	400
Assumed Width	Ft.				
Warm Inflow Speed	ft/sec	6.38	3.19	1.60	0.80
Warm Outflow Speed	ft/sec	6.38	3.19	1.60	0.80
Cold Outflow Speed	ft/sec	8.50	4.25	2.12	1.06
Warm Inflow Temperature	°F	75.7	77.2	77.9	78.6
Warm Outflow Temperature	°F	72.7	74.2	74.9	75.6
Cold Outflow Temperature	°F	45.0	45.0	45.0	45.0
Recirculation Flux	cu ft/sec	4000	1300	300	100
Warm Surface Flux	cu ft/sec	8000	10700	11700	11900
Maximum Turbulent Diffusivity	ft ² /sec	85.5	42.9	21.7	13.5
Minimum Turbulent Diffusivity Between Outflows	ft ² /sec	40.1	18.7	7.1	0.4

The warm inflow of 12000 cu ft/sec is partly warm surface flux, coming in horizontally from the surface layers of the ocean. The other part is recirculated water from the warm outflow. The table displays these two fluxes, totaling to 12000 cu ft/sec in each case. For widths 50 ft and 100 ft, the recirculation flux is substantial; for widths 200 ft and 400 ft, it is very small.

The temperature distribution at the warm inflow is lower than the ambient temperature distribution for two main reasons. The first reason is recirculation of warm outflow water (after cooling by 3°F in the evaporators); the temperature loss is proportional to the recirculation flux. The second reason is turbulent mixing with the warm outflow and with the cold outflow. We therefore present in the table the maximum turbulent diffusivity for the four cases. This maximum is reached in the cold outflow. The values near the warm inflow and outflow are only fractionally smaller in each case (see Figures 3.9 through 3.12). But the minimum value on the boundary between the outflows, is very much smaller for width 400 ft. Thus, there is significant turbulent heat transfer between the cold outflow and the surface only for the smaller widths. The table, therefore, displays the minimum value of the turbulent diffusivity on the left boundary between the outflows.

3.2. VALIDITY OF THE RESULTS

The validity of the results depends on two basic requirements:

- the numerical results are a good solution of the model problem as a system of equations; and
- the model problem is a reasonable approximation to the prototype flow conditions.

These requirements are discussed in the following two subsections.

3.2.1. Validity of the Numerical Results

The validity of the numerical results requires:

- no major coding errors;
- sufficient spatial resolution in the finite difference representations; and
- minimum error due to the remaining minor fluctuations in the solution.

First, the code is listed and documented in Part III of this report, and the different routines have been carefully analyzed. We believe the code is a faithful implementation of the equations and boundary conditions and of the numerical representations described in Part I. Although the code is fairly long, a substantial part is concerned with output, and the remainder is therefore reasonably easy to verify.

Secondly, our representation of the equations is second order in the mesh spacing. Our solutions displayed in Figures 3.1 through 3.12 do not show any significant variation on length scales smaller than a few mesh intervals. And in developing the code NRFL02, we tested carefully for dependence of the numerical results on resolution in simpler problems.

Thirdly, the numerical results for these four cases are slightly unsatisfactory because we have not completely eliminated the residual fluctuations in time. We are applying Newtonian damping to the vertical motion near the right boundary, together with a pressure boundary condition designed to ensure that fluid leaves the region at a depth agreeing with its temperature. These methods have already reduced the amplitude of the residual fluctuations to a few percent, in terms of the quantities displayed in Table 3.1. We believe that our system of equations has steady solutions, and we plan to develop numerical methods to eliminate the present fluctuations completely.

3.2.2. Validity of the Model

The validity of our model as a description of the prototype flow near the Lockheed baseline OTHF in a real ocean environment depends on the following two requirements:

- validity of the statistical turbulence model; and
- validity of the two-dimensional approximation to the Lockheed OTHF.

Neither requirement is known to be met at present. We discuss the requirements below.

Our turbulence model and parameters were chosen on the basis of our experience in stratified turbulence modeling for wake calculations, but its validity is doubtful for the present application. There is only one turbulent diffusivity, the same for each variable and for horizontal and vertical diffusion. An arbitrarily assigned constant length scale is used in the model. And the coefficients have not yet been tuned to the results of stratified turbulence experiments with inflows and outflows.

We plan to upgrade the turbulence model in the future. We will use a two-equation first-order statistical closure model, with an additional empirical equation to determine the turbulence length scale. The turbulent diffusivities will be tensors, and will use different coefficients for each variable. The effect of density stratification in impeding vertical turbulent transport will be included as in the present model. There will be a large number of unknown dimensionless parameters in the model. We plan to determine them by tuning the results against the best available experimental measurements for the statistics of stratified turbulent motions driven by inflows and outflows.

The two-dimensional NRFLO2 model of the three-dimensional flow near the prototype Lockheed baseline OTHP was described in Section 2.2. As previously stated, the approximation is substantial. The results cannot, therefore, be relied on in detail, though they are valid in order of magnitude. In a real sense, this is a baseline external flow study.

3.3. CONCLUSIONS

We draw the following conclusions from the research presented here:

1. OTHP operation in the absence of an ambient current does not raise insuperable recirculation problems. Because of the stratification, the inflows and outflows are essentially horizontal at large distances from the plant.

2. Our best estimate for the warm inflow temperature for the Lockheed OTHP, operating with the ambient temperature profile described in Section 2.4. and displayed above, is 77.5°F . This is 2.5°F below the surface temperature. Our extreme estimates were 75.7°F and 78.6°F . Changes in design, with wider, slower inflows and outflows, and with the warm inflow nearer the surface, could probably increase the warm inflow temperature up to almost the surface temperature.

3. Our numerical methods have been successfully applied in this relatively simple two-dimensional code, and we do not anticipate any insuperable problems in extending them to axisymmetric and three-dimensional codes.

ACKNOWLEDGEMENTS

This report was prepared as part of the research program, "Theoretical Fluid Dynamical Studies of Resource Availability and Environmental Impact of Ocean Thermal Power Plants", in the Naval Research Laboratory, supported by the Ocean Thermal Energy Conversion Program, Division of Solar Energy, Energy Research and Development Administration, under ERDA contract E (49-26) 1005. The majority of the work was performed under the subcontract N00014-76-C-0610 with Science Applications, Inc., and this constitutes the Final Report on that contract.

REFERENCES

1. Douglass, R. (1975), "Ocean Thermal Energy Conversion Research on an Engineering Evaluation and Test Program", Vols 1-5, TRW, Redondo Beach, Calif.
2. Piacsek, S.A., Martin, P.J., Toomre, J., Roberts, G.O. (1976), "Recirculation and Thermocline Perturbations from Ocean Thermal Power Plants", Report NRL-GFD/OTEC 2-76, Geophysical Simulation Section, Code 7750, Naval Research Laboratory, Washington, D.C.
3. Piacsek, S.A., Toomre, J., Roberts, G.O. (1975), "Geophysical Fluid Dynamics Background for Ocean Thermal Power Plants", Report NRL-GFD/OTEC 11-75, Geophysical Simulation Section, Code 7750, Naval Research Laboratory, Washington, D.C.
4. Roberts, G.O., Piacsek, S.A., Toomre, J., "Two-Dimensional Numerical Model of the Near-Field Flow for an Ocean Thermal Power Plant, Part I. The Theoretical Approach and a Laboratory Simulation", NRL-GFD/OTEC 5-76, Science Applications, Inc. and Geophysical Simulation Section, Code 7750, Naval Research Laboratory.
5. Roberts, G.O., Piacsek, S.A., Toomre, J., "Two-Dimensional Numerical Model of the Near-Field Flow for an Ocean Thermal Power Plant, Part III. Manual for the Computer Code NRFLO2", NRL-GFD/OTEC 7-76, Science Applications, Inc. and Geophysical Simulation Section, Code 7750, Naval Research Laboratory.
6. Trimble, L.C. (1975), "Ocean Thermal Energy Conversion Power Plant Technical and Economic Feasibility", Lockheed Missile and Space Co., Inc., Report NSF/RANN/SE/GI-C937/FR/75/1, Sunnyvale, Calif.